Explicit simulation of aerosol physics in a cloud-resolving model

A. M. L. Ekman, Chen Wang, J. Wilson, J. Ström

Atmos. Chem. Phys. Discuss., 4, 753–803, 2004
www.atmos-chem-phys.org/acpd/4/753/
SRef-ID: 1680-7375/acpd/2004-4-753

Atmospheric Chemistry and Physics Discussions

Explicit simulation of aerosol physics in a cloud-resolving model

A. M. L. Ekman[1], C. Wang[1], J. Wilson[2], and J. Ström[3]

[1]Massachusetts Institute of Technology, Cambridge, Massachusetts, USA
[2]Institute for Environment and Sustainability, European Commission, Ispra, Italy
[3]Institute of Applied Environmental Research, Stockholm University, Stockholm, Sweden

Received: 29 December 2003 – Accepted: 26 January 2004 – Published: 2 February 2004

Correspondence to: A. M. L. Ekman (annica@mit.edu)

Abstract

The role of convection in introducing aerosols and promoting the formation of new particles to the upper troposphere has been examined using a cloud-resolving model coupled with an interactive explicit aerosol module. A baseline simulation suggests good agreement in the upper troposphere between modeled and observed results including concentrations of aerosols in different size ranges, mole fractions of key chemical species, and concentrations of ice particles. In addition, a set of 34 sensitivity simulations has been carried out to investigate the sensitivity of modeled results to the treatment of various aerosol physical and chemical processes in the model. The size distribution of aerosols is proved to be an important factor in determining the aerosols' fate within the convective cloud. Nucleation mode aerosols ($0 \leq d \leq 5.84$ nm) are quickly transferred to the larger modes as they grow through coagulation and condensation of H_2SO_4. Accumulation mode aerosols ($d \geq 31.0$ nm) are almost completely removed by nucleation (activation of cloud droplets) and impact scavenging. However, a substantial part (up to 10% of the boundary layer concentration) of the Aitken mode aerosol population ($5.84\,\text{nm} \leq d \leq 31.0\,\text{nm}$) reaches the top of the cloud and the free troposphere. These particles may continually survive in the upper troposphere, or over time form ice crystals, both that could impact the atmospheric radiative budget. The sensitivity simulations performed indicate that critical processes in the model causing a substantial change in the upper tropospheric Aitken mode number concentration are coagulation, condensation, nucleation scavenging, nucleation of aerosols and the transfer of aerosol mass and number between different aerosol bins. In particular, for aerosols in the Aitken mode to grow to CCN size, coagulation appears to be more important than condensation. Less important processes are dry deposition, impact scavenging and the initial vertical distribution and concentration of aerosols. It is interesting to note that in order to sustain a vigorous storm cloud, the supply of CCN must be continuous over a considerably long time period of the simulation. Hence, the treatment of the growth of particles is in general much more important than the initial aerosol concentration itself.

ACPD

4, 753–803, 2004

1. Introduction

Atmospheric aerosols play a central role in cloud formation and cloud development, as particles constitute surfaces for liquid and ice particles to form. Both observational and numerical modeling studies have shown that an increase in aerosol concentrations due to anthropogenic emissions may result in optically thicker clouds and altered rainfall rates (Twomey, 1974; Albrecht, 1989; Rosenfeld, 1999; Rosenfeld, 2000). Most previous model studies in this field have focused on low-level stratiform clouds, as they cover a large part of the earth compared to other cloud types and thus are thought to have a larger impact on the Earth's climate through a change in aerosol properties. However, the few studies available on anthropogenic aerosol effects on both convective clouds and ice clouds indicate a high sensitivity of the cloud characteristics to the boundary layer aerosol concentration, and thus there is a need for additional research (Clement et al., 2002; Phillips et al., 2002; Kärcher and Lohmann, 2003).

Convective clouds provide an efficient mechanism for transporting material from the surface to the upper troposphere. Although observational data in the upper troposphere are still limited, the few measurements available all indicate the existence of high concentrations of small particles (Clarke, 1992; Clarke, 1993; Nyeki et al., 1999; Ström et al., 1999; Clarke and Kapustin, 2002; Twohy et al., 2002; Minikin et al., 2003), possibly due to the vertical transport related to deep convection. In addition, with sufficiently low temperature, high relative humidity, and relatively high concentrations of aerosol precursors; the outflow regions of convective clouds are likely areas for new aerosols to form, adding even more particles to the upper troposphere (Zhang et al., 1998; Clarke et al., 1999; Ström et al., 1999; Clement et al., 2002). However, there is still a major uncertainty regarding which chemical compounds are most important in the aerosol nucleation process, and to what extent these gases are scavenged by the heavy precipitation associated with a storm cloud.

Explicit modeling of aerosol-cloud interactions in meso-scale cloud systems is a computationally expensive task as there are numerous processes with different temporal

ACPD
4, 753–803, 2004

and spatial scales that need to be considered in simulating the cloud development; the physical and chemical properties including the size distributions of aerosols and cloud droplets, as well as the interactions among these particles. Given this broad range of conditions, most previous model studies of aerosol-cloud interactions have used simplified descriptions of the cloud processing, usually by considering adiabatic parcel models (de Reus et al., 1998; Kulmala et al., 1998a; Clement et al., 2002). Zhang et al. (1998) incorporated a two-moment aerosol model into a two-dimensional cloud and sulfate chemistry model to simulate the effects of clouds on aerosol redistribution and production in cumulonimbus clouds. They found that the nucleation rate after cloud dissipation in the upper troposphere increased by one order of magnitude compared to the nucleation rate before cloud formation. Jacobson (2003) developed a one-dimensional gas-aerosol-cloud module suitable for implementation in global or regional scale three-dimensional models. Results using this module suggest that if aerosol number is considered (i.e. mostly small particles), impact scavenging is a more important removal mechanism than nucleation scavenging, removing more than 42% of the total number of particles. On the other hand, if aerosol mass is considered (i.e. mostly large particles), nucleation scavenging is clearly the dominant aerosol removal process. These findings indicate that medium-size particles may be most likely to survive transport within a convective cloud without being scavenged by precipitation.

In order to simulate convective cloud transport along with cloud processing of aerosols, we have coupled a three-dimensional cloud-resolving model based on previous model work (Wang and Chang, 1993a; Wang and Crutzen, 1995; Wang and Prinn, 2000) with an interactive explicit aerosol module (Wilson et al., 2001). Observational data as well as weather center reanalyzed data have been used to initialize the model simulations. To evaluate the model, the results are compared with observed concentrations of aerosols and certain key chemical species, particularly in the upper troposphere (Ström et al., 1999). In this paper, only a brief evaluation of the 2-D version of the model is performed. A more detailed comparison is presented in a sequential paper (Ekman et al., manuscript in preparation) using the 3-D version of the model.

ACPD
4, 753–803, 2004

The main purpose of this research is not only to simulate the formation and transport of aerosols within as well as surrounding a convective cloud, but also to examine the sensitivity of the aerosol concentration and the properties of the cloud to various aerosol physical and chemical processes.

In this paper, we first describe the implementation of the explicit aerosol module into the cloud-resolving model. The discussions of the modeled features in dynamics, microphysics, and chemistry of the observed storm and a brief comparison between modeled and observed results are given following the model description. We then focus on the results of the sensitivity simulations aiming at revealing the dependencies of the aerosol module on various physical and chemical processes as well as initial aerosol concentration and chemical composition. The discussions and conclusions are given in the last section.

2. Model

2.1. Cloud resolving model

The cloud-resolving model (CRM) used in this study is an improved version of the model developed by Wang and Chang (1993a) with a full integration of the dynamics-physics and chemistry sub-models (Wang et al., 1995; Wang and Prinn, 2000). The dynamics-physics module consists of non-hydrostatic momentum equations, the continuity equations for water vapor and air mass density, the thermodynamic equation, and the equation of state (Wang and Chang, 1993b). Also included are prognostic equations for the mixing ratios as well as number concentrations of cloud droplets, raindrops, ice crystals and graupel particles. The microphysical transformations are formulated based on a "two-moment" scheme incorporating the size spectra of particles (Wang and Chang, 1993a; Wang et al., 1995). A δ-four-stream radiation module based on Fu and Liou (1993) is incorporated in the model and it uses predicted concentrations of gases (including H_2O and O_3) and hydrometeors to calculate radiative fluxes and

ACPD
4, 753–803, 2004

heating rates.

Cloud droplets in the atmosphere are formed on cloud condensation nuclei (CCN). In the CRM, the number of particles available for cloud droplet nucleation is predicted using the aerosol module (cf. Sect. 2.2). The number of ice nuclei (IN) is in the present model version not calculated using the explicit aerosol module. An initial IN concentration is assumed (cf. Sect. 3), and the IN are advected in the model and removed by ice particle formation, but the IN are not affected by coagulation, condensation of H_2SO_4 or other aerosol physical processes.

The chemistry sub-module predicts atmospheric concentrations of 25 gaseous and 16 aqueous (in both cloud droplets and raindrops) chemical compounds including important aerosol precursors such as sulfate and nitrate, undergoing more than 100 reactions as well as transport, and microphysical conversions. A module of heterogeneous chemistry on ice particles has been developed and is included in the present version of the model (Wang, 2004, manuscript is in preparation). This module calculates surface uptakes of several key chemical species including HNO_3, SO_2, H_2O_2 and CH_3OOH by ice particles. A selected set of surface reactions is also considered.

The cloud-resolving model has been used in studies on dynamics, microphysics, and chemistry of continental deep convection (e.g. Wang and Chang, 1993a; Wang and Chang, 1993b; Wang and Crutzen, 1995) and oceanic deep convection over the Pacific (Wang et al., 1995; Wang and Prinn, 1998; Wang and Prinn, 2000). Results obtained using the model have also been compared with available observations including aircraft, radar, and satellite data. The spatial resolution of the model can be flexibly set, a horizontal grid interval of 2 km and a vertical grid interval of 400 m are used in this study.

2.2. Aerosol module

The evolution in time and space of aerosols consisting of sulfate, organic carbon, black carbon and mixtures thereof is described using a multi-modal aerosol model (Wilson et al., 2001). In this paper, we mainly describe our revision of this module and the addi-

ACPD
4, 753–803, 2004

tional improvements needed to incorporate the aerosol module into our cloud-resolving model.

In our version of the aerosol module, five different modes are used to represent the aerosol population (Table 1). Among these five modes, carbon originating from both fossil fuel combustion and biomass burning is considered. The size distribution within each aerosol mode is assumed to be lognormal and is described by three parameters: number, mass and, standard deviation (σ_{std}). Figure 1 shows a schematic picture of the different aerosol processes treated in the model. Note that in this study, mainly to reduce the computational burden, the standard deviations are prescribed. Dry deposition of aerosols is calculated according to Langner and Rodhe (1991) using the dry deposition velocities specified in Pruppacher and Klett (1997) and Wilson et al. (2001). In the default version of the model, due to the short integration time, emissions of both carbonaceous and sulfuric aerosols are set to zero. Therefore, carbonaceous aerosols have no additional sources other than the given initial loadings during the model integration. The continuous source in addition to the given initial loading of the whole sulfuric aerosol population (three modes) is the nucleation of new sulfate aerosols from H_2SO_4 and H_2O.

New particle formation via binary H_2O-H_2SO_4 nucleation is described using the parameterization developed by Kulmala et al. (1998a). The condensation coefficient as well as the intra- and inter-modal coagulation coefficients for each aerosol mode is determined from the theory of Fuchs (1964), using the geometric mean radius of each mode. Intra-modal coagulation leads to a reduction of the number of the mode but not of the mass, whereas inter-modal coagulation leads to a reduction of the number and mass of the smaller mode and an increase of the mass of the larger mode. For the pure sulfate modes, conversions are also enforced when the upper "tail" of the mode grows beyond the prescribed size limit for a given mode (cf. Table 1). When 5% of the mass and number of aerosols is located above the size limit of the mode, then 5% is reallocated to the adjacent mode. To estimate when this mass transfer should be performed, we assume a log-normal distribution for each aerosol mode, and compare

ACPD
4, 753–803, 2004

the modeled mass weighted average diameter within each mode (diameter of average mass) with the theoretical diameter of the average mass for when the "tail" contains 5% or more of the total aerosol mass.

The activation of a drop at a certain supersaturation depends on the composition of the solute. Only a part of the aerosols in an aerosol size bin may be activated. Consider the simplified Köhler equation (e.g. Pruppacher and Klett, 1997)

$$S_{v,w} = 1 + \frac{A}{a} - \frac{B}{a^3}, \tag{1}$$

where $S_{v,w}$ is the saturation ratio, a is the droplet radius and

$$A = \frac{2M_w\sigma_{w/a}}{RT\rho_w} \quad , \tag{2}$$

$$B = \frac{3\upsilon m_s M_w}{4\pi M_s \rho_w}. \tag{3}$$

Here, M_w is the molecular weight of water and M_s is the molecular weight of the salt, $\sigma_{w/a}$ is the surface tension of water with respect to air, R is the universal gas constant, T is temperature, ρ_w is the density of water, ν is the number of ions into which a salt molecule dissociates in water and m_s is the mass of the salt.

By taking the first derivative of Eq. (1), the critical radius that corresponds to the critical saturation ratio for drop activation can be written as:

$$a^* = \sqrt{\frac{3B}{A}}. \tag{4}$$

The critical saturation ratio S^* is then obtained by inserting a^* back into Eq. (1)

$$S^* = 1 + \frac{2}{3}\sqrt{\frac{A^3}{3B}}. \tag{5}$$

ACPD
4, 753–803, 2004

The dry particle radius R is related to the variable B and we can find the critical activation radius R^*:

$$R^* = A \left[\frac{4M_s\rho_w}{27M_w\rho_s\upsilon_s(S-1)^2} \right]^{1/3}, \quad (6)$$

where ρ_s is the density of the salt, v_s is the van't Hoff dissociation coefficient (in the simulations set to 2) and S is the environmental saturation ratio. For any aerosol size bin that has R^* within its boundaries ($R_{\min} < R^* < R_{\max}$), the bin must be split so that only particles with radius larger than R^* are activated. The total number of aerosols activated can be obtained by integrating the distribution function from R^* to $R_{\max}$. Only pure sulfate aerosols and mixed aerosols are considered to constitute CCN. In many model studies, a simplified empirical relationship is used to describe droplet activation (e.g. Pruppacher and Klett, 1997):

$$N_{\mathrm{CCN}} = \mathrm{CCN} \cdot s_{v,w}^k, \quad (7)$$

where N_{CCN} is the number of activated CCN, $s_{v,w}$ is the supersaturation (%) and k is a constant varying for maritime and continental air. A sensitivity simulation is conducted to compare this traditional parameterization of aerosol activation with the description based on Koehler theory.

The activation of droplets determines the number of aerosols that are scavenged via nucleation scavenging. Another path for scavenging of aerosols is through collision with falling raindrops, graupel or ice crystals, i.e. the precipitation (impact) scavenging. The collision efficiency E in this case is by definition the probability of collisions between an aerosol and a precipitating droplet in a geometric volume swept out by the precipitating droplet in a given time interval (the droplet's effective cross-sectional area multiplied by the effective fall speed of the droplet with respect to the fall speed of the aerosol, Pruppacher and Klett, 1997). To theoretically determine E is complicated since the aerosol size varies over orders of magnitude and because the large raindrop size results in complicated flow patterns (drop oscillations, wake creation, eddy

ACPD
4, 753–803, 2004

shedding, etc.). Pruppacher and Klett (1997) present an overview of the problem. The efficiency of Brownian diffusion decreases rapidly with increasing particle size and is thus the most important removal process for small particles (diameter < 0.2 μm). Inertial impaction and interception increase in importance as the aerosol size increases. These processes are most important for particles with diameters larger than 1 μm. The previous arguments indicate that whereas there are efficient removal processes for small and large particles, the collision efficiency for particles in the 0.1 to 1.0 μm size range is relatively small. As a first attempt to simulate the variability of impact scavenging with aerosol size, different values of E for the different aerosol bins in the model are defined (Table 1). A simulation using constant E equal to 0.1 (and only for accumulation mode aerosols) is included as a sensitivity study (cf. Table 2).

Both number concentration and mass mixing ratio of the five aerosol modes, i.e. all together 10 variables, are incorporated in the cloud-resolving model as prognostic variables undergoing transport, mixing, dry deposition, and nucleation as well as precipitation scavenging besides aerosol microphysical processes. The advection scheme used to calculate the transport of these aerosol variables is the same revised Bott scheme as developed in Wang and Chang (1993a).

3. Observed case and initial model conditions

The selected case to simulate is a cumulonimbus cloud with extended anvil over northern Germany, observed during the Stratosphere-Troposphere Experiment by Aircraft Measurements (STREAM) on 29 July 1994 (Ström et al., 1999). Convection was initiated as cool air from the Atlantic Ocean was advected towards Western Europe after several weeks of stagnant weather with clear skies, high temperatures and weak winds. During the preceding high-pressure period, a build-up of high boundary layer concentrations of aerosol particles, CO and O_3 had occurred. Several smaller groups of thunderstorms were formed along the cold front, and the aircraft measurements were conducted along a cross-section through the center of one of these storm clouds.

ACPD
4, 753–803, 2004

During the measurement flight, particles smaller than 1 μm diameter were sampled and counted using two TSI-3760 CPCs with lower cutoffs at 0.007 and 0.018 μm diameter, respectively. Note that the former cutoff of the particle counter is about 0.0015 μm smaller than the upper limit of size of what is termed "the Aitken mode sulfate aerosol" in our model. A counterflow virtual impactor (CVI) was used to sample cloud particles larger than ~5μm aerodynamic diameter. Water vapor was measured using a Lyman-α absorption hygrometer and observations of carbon monoxide and ozone mixing ratios were performed using the laser diode technique and chemiluminescence technique, respectively. The aircraft measurements were carried out in the anvil region of the storm. The research aircraft entered the cumulonimbus cloud at approximately 14:36 UTC at an altitude of ~10 400 m. The aircraft flew a distance of ~260 km across a frontal zone before leaving the cloudy air at about 15:03 UTC. In situ data from this level are presented in Fig. 5 in Ström et al. (1999).

The meteorological part of the CRM simulation is initialized using analyzed 3-dimensional initial data fields of pressure, temperature, winds and specific humidity obtained from the National Centers for Environmental Prediction (NCEP). Horizontally interpolated fields of NO_2, NO_3, O_3, SO_2 and SO_4 obtained from surface observations conducted by the Co-operative Programme for Monitoring and Evaluation of the Long-Range Transmission of Air Pollutants in Europe (EMEP, Hjellbrekke and Hanssen, 1998) are used to initialize the chemistry module. Vertical profiles of these species are prescribed as to decrease with height except for O_3, which is based on previous work.

For Aitken, black carbon, and mixed mode aerosols, a horizontally constant surface concentration of 50 cm^{-3} is assumed initially. The surface concentration of accumulation mode aerosols is set to be 500 cm^{-3}. For ice nuclei particles (IN), the initial surface concentration is set to be 100 cm^{-3}. These aerosol concentrations represent values typically observed in urban continental air (Seinfeld and Pandis, 1998). All aerosol concentrations are initially prescribed to decrease with height as a function of air density (surface concentration multiplied by $[\rho_{level}/\rho_{surface}]^3$, cf. Fig. 2). The nucleation mode aerosol concentration is assumed to be zero at the beginning of the simulation.

ACPD
4, 753–803, 2004

4. Results

In order to evaluate the behavior of the aerosol module incorporated into the cloud-resolving model and to explore the dependencies of this module on various physical and chemical processes as well as on initial aerosol concentrations and chemical compositions, we have designed 34 sensitivity simulations. These sensitivity simulations, targeting various physical and chemical parameters or processes, are categorized into 8 groups, hereafter labeled as A1 to H4 (cf. Table 2).

To achieve computational efficiency, we make use of the two-dimensional version of our model in the sensitivity simulations. Results obtained using the 2-D version of the model may slightly differ compared to the 3D-simulation results (not shown in this paper), as the 2-D model version only simulates the cloud development along a cross-section of the convective cloud. For example, a comparison between the two model versions shows that the depth and the extension of the simulated anvil are not identical. However, for examining the sensitivity of the model this difference should not be of major importance.

The 2-D simulations are carried out over a 150×50 grid domain, covering 300 km horizontally and 20 km vertically. The 2-D chemical compound and meteorology fields used for the initialization of the model are cross-sections extracted from the thermodynamically most unstable area of the previously described 3-D initial fields (cf. Fig. 3). Open boundary conditions are applied for all variables, i.e. the influx to the model domain is equal to zero. Starting time is 12:00 UTC and the simulation is integrated for 3 h. Each time step is 5 s.

4.1. Reference simulation

A reference run was first designed for the sensitivity study. The purpose of this reference run is mainly to provide a "baseline" result that is in agreement with observational data for comparison with the rest of the sensitivity tests.

The characteristics of the simulated storm development are displayed in Fig. 4. Fig-

ACPD
4, 753–803, 2004

ure 5 shows the 2-dimensional distribution of various model parameters after 3 h of simulation. Available observed maximum values at ~10.4 km of cloud water content (CWC), crystal number density (CND), condensation nuclei (radius >7 nm, CN), and mixing ratios of CO and O_3 are indicated in the figures. Modeled maximum values at 10.4 km of CWC, CND, CO and O_3 differ less than 20% from the observations. Note that modeled and observed parameters at the same altitude level may not correspond exactly to each other; they should rather be considered as representative values of the cloud anvil.

As mentioned in Sect. 3, the weather before the passage of the cold front on July 29 had given rise to enhanced boundary layer concentrations of aerosol particles, CO and O_3. Figure 5d displays that high concentrations of Aitken mode aerosol particles are rapidly transported from the surface up to the free troposphere within the convective cloud. The simulated concentration at 10.4 km altitude is about two times higher than the observed one. However, the measurements only consider particles with a radius larger than 7 nm, whereas the Aitken mode size interval includes all particles with a radius larger than 6 nm. If a log-normal size distribution is assumed and the upper 'tail' of the particles between 6 and 7 nm is removed, the modeled maximum particle concentration at 10.4 km is reduced to 2.4×10^4 cm^{-3}, which corresponds very well with the observations.

The transport of high concentrations of CO and SO_2 from the boundary layer to the top of the cloud can clearly be seen in Figs. 5h and 5j. For O_3, high concentrations in the free troposphere are usually a result of downward transport of O_3 rich air from the stratosphere. However for the present case, a plume of polluted air with elevated O_3 concentrations close to the surface is transported from the eastern boundary of the model to the free troposphere (cf. Fig. 5i).

The sensitivity of the modeled results to a given parameter or process is judged by the relative difference between the results of the given sensitivity simulation and the corresponding values of the reference run. Model variables used in the comparison include the concentration of Aitken mode sulfate aerosols as well as mixing ratios of

ACPD
4, 753–803, 2004

CO and SO_2 in the upper troposphere (where observations of aerosol number and CO are available), and surface precipitation, representing several aspects of interest dealing with aerosol microphysics, convective transport of important trace gases, as well as cloud dynamics and microphysics. It is worthwhile noting that our sensitivity simulations are carried out using a "real" atmospheric case rather than an idealized case of deep convection. The impact of the tested parameters or processes on the interactions among aerosols, cloud droplets, and cloud dynamics thus are included.

4.2. Aerosol microphysics (Experiment A, F and H)

In the aerosol module, the accumulation mode sulfate aerosol, which serves as the major part of CCN in the model, mainly originates from coagulation and condensation of Aitken mode aerosols. The concentration of Aitken mode aerosols is determined by the rates of aerosol nucleation, condensation and coagulation involving nucleation mode aerosols. In order to explore the sensitivity of the modeled results to these processes, we have designed the A series with coagulation, condensation, or both coagulation and condensation processes being switched off; the F series with reduced nucleation rate; and the H series with altered or no transfer between the various modes.

It is found that the largest change in Aitken mode number concentration (MNC) at 10.4 km occurs when no coagulation or transfer between the different modes is considered, or when the size limit for transfer between the modes is increased (case A1, A2, H1 and H3; Fig. 6a). The main pathway for Aitken mode aerosol to CCN appears to be coagulation, as the concentration of Aitken mode particles in the upper troposphere is higher compared to the reference case in case A1 (Fig. 6a). An increase in the Aitken MNC cannot be seen if only condensation of H_2SO_4 on the aerosols is excluded. Switching off coagulation leads to a decrease of the total ice/droplet number concentration (Fig. 6b) since the aerosols in Aitken mode are too small to constitute CCN.

For all A cases as well as the H1 and H2 simulations, not enough CCN are produced from the Aitken mode to sustain a vigorous storm cloud. Thus, the average

ACPD
4, 753–803, 2004

accumulated precipitation (Fig. 6d) is reduced and vertical wind speeds are substantially weaker than the reference run results. As a consequence of the weak storm development, the mixing ratios of both CO and SO_2 in the upper troposphere are lower than those of the reference simulation (Figs. 6e and 6f). The convection is also less developed for the H4 case (10% mass transfer between the modes instead of 5%) compared to the reference run and the precipitation and transport of trace gases to the free troposphere is just as weak as in the A simulations.

For the H3 case on the contrary, when particles are allowed to be transferred more rapidly from Aitken to accumulation mode compared to the reference case, the convection becomes more intense. As seen in Fig. 6c the droplet number concentration at 4.0 km is accordingly higher in this case than in the reference simulation. Vertical wind speeds are stronger and thus more SO_2 and CO is transported vertically compared to the reference case results. However, the Aitken MNC at 10.4 km is lower compared to the reference case, as more particles are scavenged through nucleation scavenging within the convective cloud in case H3.

A decrease in the aerosol nucleation rate by a factor of two (case F1) affects the average upper tropospheric Aitken MNC substantially. The convective cloud is less developed in this case compared to the reference case and the transport of trace gases to the free troposphere is weaker. If the nucleation rate is reduced by a factor of 10 (case F2), the average Aitken MNC at 10.4 km decreases by approximately 40%. Surprisingly, we have found in these model simulations that the decrease in Aitken MNC was not caused by weaker convection and vertical wind speeds, but instead by stronger convection and thus more efficient nucleation and impact scavenging (the average precipitation increases compared to the reference case). When fewer nucleation mode particles are produced, more H_2SO_4 is available, and the growth of nucleation and Aitken mode aerosols to CCN due to condensation becomes very efficient. As seen in Fig. 6b, the particle/droplet number concentration at 10.4 km is also higher in the F2 case compared to the reference simulation. The convection is more intense in the F3 case, where the nucleation rate is increased by one order of magnitude. There is a

considerable change in the Aitken MNC in the free troposphere and also in droplet/ice particle number concentration in this case.

4.3. Aerosol dry deposition (Experiment B)

The results of series B (dry deposition, Fig. 7) suggest that the modeled Aitken MNC at 10.4 km is not particularly sensitive to the formulation of dry deposition of aerosols. Modeled average Aitken MNCs differ less than 10% compared to the reference simulation. The convection is slightly stronger in the B1 case where more CCN are available, resulting in increased transport of trace gases to the free troposphere and more precipitation. In the B2 case, the vertical wind speed within the convective cloud is somewhat lower compared to the reference case and the transport of trace gases to the free troposphere is reduced. However, the horizontal and vertical extent of the cloud is about the same as for the reference simulation and the total average precipitation actually increases by ~40%.

4.4. Aerosol scavenging processes (Experiment C and E)

Once the cloud starts to develop, the scavenging of aerosols via nucleation scavenging (aerosols activated to form cloud droplets) or by impact scavenging (aerosols removed by precipitating particles) will influence the upper tropospheric concentration of aerosols. We have tested the sensitivity of the modeled results to various setups in the scavenging calculations.

In sensitivity series C (Fig. 8), different collision coefficients (cases C1 to C4 and C6 to C7) along with additional impact scavenging of BC aerosols (case C5) are tested. The change in average Aitken MNC in the free troposphere is the largest when the impact scavenging is removed completely (C4). However, even in this case, the change in Aitken MNC is only slightly more than 10% compared to the reference case. Despite the small changes in Aitken MNC, the shape of the cloud clearly differs among the C cases and the reference simulation, resulting in a change of the average precipitation

amount by up to 50%. In addition, as can be seen in Fig. 8c, the average droplet concentration at the cloud base (which is mainly affected by the number of CCN) is changed by up to 100%.

It is interesting to note that for the two cases with lower collision efficiency than in the reference case, the convection turns out to be less intense with reduced vertical wind speeds. Accordingly, the concentration of trace gases at 10.4 km is lower; the difference is up to 15% for CO and up to 40% for SO_2. The insensitivity of upper tropospheric Aitken MNCs to different treatments of impact scavenging is not entirely a surprise. Kinetically speaking, the collection efficiency of aerosols, particularly those in the size range of Aitken mode, by precipitating particles is very low (Table 1; see also Pruppacher and Klett, 1997).

The usage of a new aerosol module in the CRM (cf. Sect. 2.2) introduces the possibility to calculate size-dependent nucleation of cloud droplets. This method has been compared with the method using an empirically derived formula in experiment E1. The sensitivity of the size-dependent nucleation on the calculation of the critical activation radius is tested in series E2-E5. In the case where the critical activation radius is 10 times smaller compared to the reference case (E3), a larger fraction of Aitken mode particles are considered as CCN and thus scavenged in the nucleation of cloud droplets. Hence, the average Aitken MNC at 10.4 km decreases by almost 90%. For the other E cases, the changes in average Aitken MNC is small. The shape and the extent of the cloud are clearly different for all E cases compared to the reference case and the average precipitation rate either increases (E3 and E4) or decreases (E1–E2, E5) by 20% or more. In both the E1 and E2 cases there is also a substantial decrease in the average droplet/particle concentration at 10.4 km. This suggests the empirical method commonly used in cloud-resolving models for calculating nucleation of cloud droplets underestimates the nucleation-scavenging rate of aerosol. For the E3 case, where the convection is more intense compared to the reference case, there is a considerably stronger transport of trace gases to the free troposphere.

ACPD
4, 753–803, 2004

4.5. Initial distribution of aerosols (Experiment D)

The sensitivity of the model to the initial distribution and concentration of aerosols is tested in experiments D1-D8 (Fig. 9). The modeled average precipitation increases substantially in case D3 and D6 (where the decrease of the aerosol number concentration with height is either removed or reduced) whereas it decreases in cases D2, D4, D5 and D7. For cases D1, and D8 the change is small.

In simulations D2 and D5, where the particles are larger and fewer compared to the reference simulation, the convective activity is limited and vertical wind speeds are low. In case D7, where more Aitken mode particles are available initially, the convection is also less developed compared to the reference case because of inefficient coagulation and condensation caused by high particle number in this case. Compared to the reference case, average trace gas concentrations at 10.4 km decrease up to 20% for CO and 45% for SO_2. However, the Aitken MNC at 10.4 km is not substantially altered by the change in precipitation and vertical wind speeds within the cloud. Differences are less than 10%.

The fact that the Aitken MNC at 10.4 km after 3 h of simulation is almost unaffected by the choice of initial aerosol profile suggests that the chemical and physical conversions taking place within a convective cloud are very fast, and the changes in Aitken mode aerosol properties in the upper troposphere are mainly influenced by these rapid conversions, not the initial conditions. Already at an early stage of the simulation, accumulation mode and Aitken mode aerosols are scavenged by intense precipitation. Hence, the concentration of particles after 3 h of simulation is more determined by the formation and growth of small particles than by the initial concentration of CCN.

It is also interesting to note that, despite the small change in Aitken MNC, the average droplet/particle number concentration at 10.4 km changes by over 10% in a majority of the D simulations. The explanation may be that the ice nuclei number is not calculated using the explicit aerosol module (cf. Sect. 2.2). Hence, processes that will have a crucial influence on the number of ice crystals formed are e.g. upwind velocity, relative

ACPD
4, 753–803, 2004

humidity and temperature and not the Aitken MNC.

4.6. Initial concentration of aerosol precursor (Experiment G)

The simulated nucleation rate of aerosols is determined by the modeled temperature, relative humidity and H_2SO_4 concentration. Nucleation mode particles grow rapidly to become Aitken mode and then accumulation mode particles and they may hence be a major source of CCN. The G series of experiments are designed to examine the sensitivity of the model to the initial H_2SO_4 concentration (Fig. 10).

For the G1 case, where more H_2SO_4 is available initially, the convection is more intense compared to the reference case and more particles are scavenged by precipitation, resulting in a lower average Aitken MNC at 10.4 km. The average accumulated precipitation over the model domain is similar as for the reference case, but the precipitation is more widespread and the precipitation maximum substantially lower. There is also a significant increase in the droplet concentration close to the cloud base.

For the G2 case, less H_2SO_4 is available at the beginning of the simulation and fewer nucleation mode particles are formed. The convection is less intense and both the average and maximum precipitation rate substantially lower. The transport of Aitken mode particles to the free troposphere is weaker compared to the reference case. Lower vertical wind speeds also result in lower trace gas concentrations at 10.4 km. For both G cases, the total condensed H_2SO_4 after 3 h of simulation is almost unaffected.

4.7. Hydrometeor properties

Besides the upper tropospheric distributions of aerosols and chemical species, the characteristics of the cloud droplets and precipitation particles can also be changed by altered descriptions of physical and chemical processes. Figure 11 shows various hydrometeor characteristics for a selected number of sensitivity simulations (the selected cases are the ones where a clear difference in the Aitken MNC at 10.4 km compared to the reference case was obtained, as well as the case where the initial Aitken MNC

ACPD
4, 753–803, 2004

was increased by a factor of 100).

Close to the cloud base (at 2 km), the average drop radius over 3 h of simulation is approximately 20μm for the reference simulation. The largest change in cloud droplet size is obtained in the A2 simulation where no coagulation or condensation is considered. In this case, the average droplet radius is ~45μm. Fewer particles are available as CCN and hence the existing droplets may grow larger.

The smallest cloud droplets are found in the E3 and H3 cases. In both these simulations, more CCN are available compared to the reference simulation and the average droplet radius decreases to 14 and 16μm, respectively. The average drop radius for rain at the lowest model level (400 m) is also smaller in the E3 and H3 simulations. Compared to the reference case, the falling raindrops below the cloud decrease by 37% and 7%, respectively. Consistently with this result, rain drops higher up in the cloud (e.g. at 7.2 km), are in the E3 and H3 simulations smaller (23% and 5%) than in the reference simulation and graupel particles at 8 km altitude are also smaller.

At the top of the cloud, the simulated ice particles are actually slightly larger over the 3 h simulation period in the E3 and H3 cases compared to the reference case. Fewer Aitken mode particles are transported to the top of the cloud, and the ice particles can grow more efficiently. This result is in contrast with the findings by e.g. Sherwood (2002) who using satellite-retrieved data found a negative correlation between aerosol amounts and ice crystal radius at the top of convective clouds.

The onset of the rain occurs at about the same time in all of the simulations. It starts somewhat later in simulations A1, A2, D5, G2, H1 and D7 than in the reference simulation. In all of the sensitivity simulations where the onset of the rain is later compared to the reference simulation, there are generally fewer particles available to constitute CCN, the cloud is less developed, and the rain also terminates sooner. One exception is the D7 case, where actually more Aitken mode particles are available at the beginning of the simulation. In this case, the particles with smaller sizes are so numerous that they cannot grow efficiently to become CCN. For the D1, E3 and H3 simulations, where more CCN are available throughout the simulation and the convection is more

ACPD
4, 753–803, 2004

intense, the graupel and ice formation thus occur earlier than in the reference simulation.

5. Conclusions

The role of convection in introducing aerosols and promoting the formation of new particles to the upper troposphere has been examined using a cloud-resolving model coupled with an interactive explicit aerosol module. The size distribution of aerosols is an important factor in determining the aerosols' fate within the convective cloud. Accumulation mode aerosols, as ideal CCN, are removed almost completely by the heavy precipitation within the modeled storm cloud. Nucleation mode aerosols grow fast due to coagulation and condensation and are in addition efficiently scavenged by falling precipitating droplets. Hence, there is only a small part of the population (concentrations of a few particles per cm^{-3}) that reaches the free troposphere. Aitken mode aerosols are to some extent removed by nucleation scavenging, but the particles in the lower part of the size range are not efficient as CCN and are thus transported to the top of the storm cloud. Once in the free troposphere, Aitken mode particles may grow over time and are eventually available as IN. In the model simulations, up to 10% of the Aitken mode particles in the boundary layer reach the anvil of the cloud.

A set of 34 sensitivity simulations performed, using various physical and chemical settings as well as different initial aerosol concentrations and chemical compositions, indicates that critical processes in the model causing a substantial change in the upper tropospheric Aitken MNC (between ten and several hundred percent) are coagulation, condensation, nucleation scavenging, nucleation of aerosols and also the transfer of aerosol mass and number between different aerosol bins. Less important processes are dry deposition, impact scavenging and the initial vertical distribution and concentration of aerosols.

Coagulation is the major pathway in the model for production of Aitken mode particles. When this process is shut off, the production of CCN is reduced by several orders

ACPD
4, 753–803, 2004

of magnitude. No vigorous convection is initiated as a result, which means that condensation of H_2SO_4 onto particles cannot alone produce enough new CCN. Omitting condensation in the model also results in a slower growth of small particles and the convection becomes weaker than in the reference simulation, but not as weak as if coagulation is left out of the model.

The simulation of nucleation scavenging in the present model version is size-dependent, and the calculation of the critical radius for activation of particles appears to be of major importance to the modeled results. If the critical activation radius is decreased by a factor of 10 in the model, the characteristics of the cloud becomes substantially different and the Aitken MNC in the free troposphere decreases by 89% compared to the reference case. In addition, use of the empirical method for the calculation of nucleation scavenging leads to a decrease of the Aitken MNC at 10.4 km by more than 10%.

The present study shows that the parameterized rate of nucleation clearly affects both the upper tropospheric Aitken MNC and ice particle/droplet number concentration (and hence the overall cloud development). Atmospheric nucleation is still a poorly known process. It has e.g. been shown that observed nucleation rates frequently exceed those predicted by sulfuric acid-water nucleation theories and laboratory measurements (Weber et al., 1997; Covert et al., 1992; Viisanen et al., 1997; Clarke et al., 1998; Kulmala et al., 1998b; O'Dowd et al., 1999; Birmili and Wiedensohler, 2000).

Due to the possible overlap of different modes of aerosols, "remapping" aerosol size distribution by allowing transfer of aerosols from one mode to another is a common and necessary procedure in aerosol models of modal type. The set of sensitivity simulations aiming at the transfer of particles between the different sulfate modes indicate that certain degree of cautiousness should be applied for this procedure. Even a relatively small change in assumed mass transfer limit (from 5% to 10% in the related sensitivity tests) might cause significant changes in modeled results including the upper tropospheric redistributions of Aitken mode aerosols and chemical compounds. In addition, the transfer of aerosol particles is dependent on the calculation of the diameter of aver-

age mass (which determines the shape of the distribution function) and an error in this calculation by a factor of two causes substantial changes in the cloud development.

Recent studies (Sherwood, 2002; Phillips et al., 2002) have suggested a negative correlation between ice crystal size at the top of a convective cloud and aerosol loading close to the ground. In the present study, the simulated ice particles in the free troposphere are actually somewhat larger if the aerosol concentration in the boundary layer is high. However, the average radius of cloud droplets, rain droplets and graupel particles becomes smaller. In the present model, the aerosol module does not give the number of available particles for ice nucleation (cf. Sect. 2.2). Hence, the growth of ice crystals in the upper part of the cloud is more dependent on the vertical velocity, temperature and most importantly water vapor supply, than on the by the aerosol module calculated aerosol concentration in the boundary layer. For future studies, the number of available ice nuclei will just as the number of CCN be predicted by the aerosol module.

A noticeable variation in the development and characteristics of the convection has been found in all of the sensitivity simulations. In order to sustain a vigorous storm cloud, the supply of CCN must be continuous over a considerably long period during the simulation. Hence, the treatment of the growth of particles is in general much more important than the initial aerosol concentration itself. However, it is also crucial that enough CCN are available at the beginning of the simulation for the actual initiation of the convection. Otherwise, the cloud development becomes slow, vertical wind speeds weak and precipitation amounts low.

Acknowledgements. The first author would like to thank the Knut and Alice Wallenberg foundation postdoctoral fellowship program on sustainability and the environment, Sweden, for research funding. This work was also partially supported by the NOAA Climate and Global Change Program grant GC97-474 and by the industrial consortium of the MIT Joint Program on the Science and Policy of Global Change.

References

Albrecht, B. A.: Aerosols, cloud microphysics, and fractional cloudiness, Science, 245, 1227–1230, 1989.

Birmili, W. and Wiedensohler, A.:New particle formation in the continental boundary layer: Meteorological and gas phase parameter influence, Geophys. Res. Lett., 27, 20, 3325–3328, 2000.

Clarke, A. D.: Atmospheric nuclei in the remote free troposphere, J. Atmos. Chem., 14, 1–4, 479–488, 1992.

Clarke, A. D.: Atmospheric nuclei in the Pacific midtroposphere: Their nature, concentration, and evolution, J. Geophys. Res., 92, 10 633–20 647, 1993.

Clarke, A. D., Davis, D., Kapustin, V. N., Eisele, F., Chen, G., Paluch, I., Lenschow, D., Brandy, A. R., Thornton, D., Moore, K., Mauldin, L., Tanner, D., Litchy, M., Carroll, M. A., Collins, J., and Albercook, C.: Particle nucleation in the tropical boundary layer and its coupling to marine sulfur sources, Science, 282, 5386, 89–92, 1998.

Clarke, A. D., Eisele, F., Kapustin, V. N., Moore, K., Tanner, D., Mauldin, L., Lichty, M., Lienert, B., Carrol, M. A., and Albercook, G.: Favorable environments during PEM-Tropics, J. Geophys. Res., 104, D5, 5735–5744, 1999.

Clarke, A. D. and Kapustin, V. N.: A pacific aerosol survey, Part I: A decade of data on particle production, transport, evolution, and mixing in the troposphere, J. Atmos. Sc., 59, 4, 363–382, 2002.

Clement, C. F., Ford, I. J., Twohy, C. H., Weinheimer, A., and Campos, T.: Particle production in the outflow of a midlatitude storm, J. Geophys. Res.-Atmos., 107, D21, Art. No. 4559, 2002.

Covert, D. S., Kapustin, V. N., Bates, T. S., and Quinn, P. K.: New particle formation in the marine boundary layer, J. Geophys. Res.-Atmos., 97, 20 581–20 589, 1992.

de Reus, M., Ström, J., Kulmala, M., Prijola, L., Lelieveld, J., Schiller, C., and Zöger, M.: Airborne aerosol measurements in the tropopause region and the dependence of new particle formation on preexisting particle number concentration, J. Geophys. Res., 103, 31 255–31 263, 1998.

Fu, Q. and Liou, K. N.: Parameterization of the radiative properties of cirrus clouds, J. Atmos. Sc., 50, 2008–2025, 1993.

Fuchs, N. A.: The mechanics of aerosols, Pergamon Press, Oxford, 1964.

Hjellbrekke, A. G. and Hanssen, J. E.: Data report 1996, Part 2, Monthly and seasonal sum-

maries, The Norwegian Institute for Air Research, Lillestrom, Norway, NILU/CCC-report 2/98, 229, 1998.
Jacobson, M. Z.: Development of mixed-phase clouds from multiple aerosol size distributions and the effect of the clouds on aerosol removal, J. Geophys. Res.-Atmos., 108, D8, Art. No. 4245, 4:1–4:23, 2003.
Kärcher, B. and Lohmann, U.: A parameterization of cirrus cloud formation: Heterogeneous freezing, J. Geophys. Res.-Atmos., 108, D14, Art. No. 4402, 2:1–2:152003.
Kulmala, M., Laaksonen, A, and Pirjola, L.: Parameterizations for sulphuric acid/water nucleation rates, J. Geophys. Res., 103, 8301–8307, 1998a.
Kulmala, M., Toivonen, A., Mäkelä, J. M., and Laaksonen, A.: Analysis of the growth of nucleation mode particles observed in Boreal forest, Tellus Series B-Chemical and Physical Meteorology, 50, 449–462, 1998b.
Langner, J. and Rodhe, H.: A global three-dimensional model of the tropospheric sulfur cycle, J. Atmos. Chem., 13, 225–263, 1991.
Minikin, A., Petzold, A., Ström, J., Krejci, R., Seifert, M., van Velthoven, P., Schlager, H., and Schumann, U.: Aircraft observations of the upper tropospheric fine particle aerosol in the Northern and Southern Hemispheres at midlatitudes, Geophys. Res. Lett., 30, 10, Art. No. 1503, 10:1–10:4, 2003.
Nyeki, S., Kalberer, M., Lugauer, M., Weingartner, E., Petzold, A., Schroder, F., Colbeck, I., and Baltensperger, U.: Condensation Nuclei (CN) and Ultrafine CN in the Free Troposphere to 12 km: A case study over the Jungfraujoch high-alpine research station, Geophys. Res. Lett., 26, 14, 2195–2198, 1999.
O'Dowd, C., McFiggans, G., Creasey, D. J., Pirjola, L., Hoell, C., Smith, M. H., Allan, P. J., Plane, J. M. C., Heard, D. E., Lee, J. D., Pilling, M. J., and Kulmala, M.: On the photochemical production of new particles in the coastal boundary layer, Geophys. Res. Lett., 26, 12, 1707–1710, 1999.
Phillips, V. T. J., Choularton, T. W., Blyth, A. M., and Latham, J.: The influence of aerosol concentrations on the glaciation and precipitation of a cumulus cloud, Quarterly Journal of the Royal Meteorological Society, 128 581, 951–971, 2002.
Pruppacher, H. R. and Klett, J. D.: Microphysics of clouds and precipitation, Klüwer Academic Publishers, Dordrecht, The Netherlands, 1997.
Rosenfeld, D.: TRMM Observed First Direct Evidence of Smoke from Forest Fires Inhibiting Rainfall, Geophys. Res. Lett., 26, 20, 3105–3108, 1999.

Rosenfeld, D.: Suppression of rain and snow by urban and industrial air pollution, Science, 287, 1793–1796, 2000.
Seinfeld, J. H. and Pandis, S. N.: Atmoshperic chemistry and physics: From air pollution to climate change, 1326, John Wiley & Sons, inc., 1998.
Sherwood, S.: A microphysical connection among biomass burning, cumulus clouds, and stratospheric moisture, Science, 295, 5558, 1272–1275, 2002.
Ström, J., Fischer, H., Lelieveld, J., and Schröder, F.: In situ measurements of microphysical properties and trace gases in two cumulonimbus anvils over western Europe, J. Geophys. Res., 104, 12 221–12 226, 1999.
Twohy, C. H., Clement, C. F., Gandrud, B. W., Weinheimer, A. J., Campos, T. L., Baumgardner, D., Brune, W. H., Faloona, I., Sachse, G. W., Vay, S. A., and Tan. D.: Deep convection as a source of new particles in the midlatitude upper troposphere, J. Geophys. Res.-Atmos., 107, D21, Art. No. 4560, 6:1–6:10, 2002.
Twomey, S.: Pollution and the planetary albedo, Atmos. Env., 8, 1251–1256, 1974.
Viisanen, Y., Kulmala, M., and Laaksonen, A.: Experiments on gas-liquid nucleation of sulfuric acid and wafer, J. Chem. Phys., 107, 4, 920–926, 1997.
Wang, C. and Chang, J. S.: A three-dimensional numerical model of cloud dynamics, microphysics, and chemistry, 1, Concepts and formulation, J. Geophys. Res., 98, D8, 14 827–14 844, 1993a.
Wang, C. and Chang, J. S.: A three-dimensional numerical model of cloud dynamics, microphysics, and chemistry: 4. Cloud chemistry and precipitation chemistry, J. Geophys. Res., 98, D9, 16 799–16 808, 1993b.
Wang, C. and Crutzen, P. J.: Impact of a simulated severe local storm on the redistribution of sulfur dioxide, J. Geophys. Res., 100, D6, 11 357–11 367, 1995.
Wang, C., Crutzen, P. J., Ramanathan, V., and Williams, S. F.: The role of a deep convective storm over the tropical Pacific Ocean in the redistribution of atmospheric chemical species, J. Geophys. Res., 100, D6, 11 509–11 516, 1995.
Wang, C. and Prinn, R. G.: Impact of the horizontal wind profile on the convective transport of chemical species, J. Geophys. Res., 103, D17, 22 063–22 071, 1998.
Wang, C. and Prinn, R. G.: On the roles of deep convective clouds in tropospheric chemistry, J. Geophys. Res., 105, D17, 22 269–22 297, 2000.
Weber, R. J., Marti, J. J., McMurry, P. H., Eisele, F. L., Tanner, D. J., and Jefferson, A.: Measurements of new particle formation and ultrafine particle growth rates at a clean continental

site, J. Geophys. Res.-Atmos., 102, D4, 4375–4385, 1997.
Wilson, J., Cuvelier, C., and Raes, F.: A modeling study of global mixed aerosol fields, J. Geophys. Res.-Atmos., 106, D24, 34 081–34 108, 2001.
Zhang, Y. P., Kreidenweis, S., and Taylor, G. R.: The effects of clouds on aerosol and chemical species production and distribution. Part III: Aerosol model description and sensitivity analysis, J. Atmosp. Sc., 55, 7, 921–939, 1998.

Table 1. Diameter, standard deviation and collision efficiency of aerosol module modes.

	Dry count geometric diameter size interval (μm)	Geometric standard deviation (σ_{std})	Collision efficiency[1] estimated lower/higher limits are given within parenthesis
Nucleation mode SO_4	0–0.00854	1.59	0.5 (0.5/0.5)
Aitken mode SO_4	0.00854–0.031	1.59	0.06 (0.0075/0.125)
Accumulation mode SO_4 for r$\leq$2.5 μm	>0.031	1.59	0.025 (0.0075/0.075) for r<0.1 μm, 0.0075 (0.0001/0.01) for r<1.0 μm, 0.05 (0.0025/0.075) for r<2.5 μm, 1.0 (1.0/1.0)
Pure BC	–	2.0	–
Mixed BC/OC/SO_4	–	2.0	Same as for accumulation mode SO_4

[1] Based upon values given in Figure 17-17 in Pruppacher and Klett (1997).

ACPD
4, 753–803, 2004

Table 2. Summary of sensitivity simulations conducted using the CRM.

Simulation number	Simulation name	Characteristics
1	R	Reference simulation
2	A1	No coagulation of aerosols
3	A2	No coagulation, no condensation of H_2SO_4 on aerosols
4	A3	No condensation of H_2SO_4 on aerosols
5	B1	No dry deposition of aerosols
6	B2	10 times higher dry deposition velocity for all aerosols
7	C1	Constant collision efficiency constant
8	C2	Collision efficiency multiplied by 2.
9	C3	Collision efficiency divided by 2.
10	C4	No impact scavenging of aerosols
11	C5	Impact scavenging of BC included (in same manner as for acc. mode SO_4)
12	C6	Lower limit of impact scavenging (cf. Table 1)
13	C7	Higher limit of impact scavenging (cf. Table 1)
14	D1	Aerosol initial number concentration (but not mass) multiplied by 2 throughout the whole model domain
15	D2	Aerosol initial number concentration (but not mass) divided by 2 throughout the whole model domain
16	D3	Constant initial aerosol concentration throughout the whole model domain (surface concentration used for all aerosols, instead of decreasing concentration with altitude scaled by density)
17	D4	Aerosol initial mass concentration multiplied by 2 throughout the whole model atmosphere
18	D5	Aerosol initial mass concentration divided by 2 throughout the whole model atmosphere

ACPD
4, 753–803, 2004

Table 2. Continued.

Simulation number	Simulation name	Characteristics
19	D6	Altered vertical slope of initial aerosol distribution (surface concentration multiplied by $(\rho_{level}/\rho_{surface})^{1.5}$ instead of $(\rho_{level}/\rho_{surface})^{3}$)
20	D7	Initial Aitken number concentration multiplied by 100 throughout the whole model domain
21	D8	Initial BC number concentration multiplied by 10 throughout the whole model domain
22	E1	Old nucleation scavenging parameterization (cf. Eq. 5)
23	E2	10 times larger critical radius (cf. Eq. 4)
24	E3	10 times smaller critical radius (cf. Eq. 4)
25	E4	Halved nucleation scavenging over the whole model domain
26	E5	SO4 used for aerosol density instead of $(NH_4)_2SO_4$ (in Eq. 4)
27	F1	Aerosol nucleation decreased by a factor of 2 over the whole model domain
28	F2	Aerosol nucleation decreased by a factor of 10 over the whole model domain
29	F3	Aerosol nucleation increased by a factor of 10 over the whole model domain
30	G1	10 times higher initial H_2SO_4 concentration (up to 4 km altitude)
31	G2	10 times lower initial H_2SO_4 concentration (up to 4 km altitude)
32	H1	No transfer of aerosols between the modes
33	H2	2 times larger radius for transfer (cf. Sect. 2.2)
34	H3	2 times smaller radius for transfer (cf. Sect. 2.2)
35	H4	10% transfer of mass instead of 5% (cf. Sect. 2.2)

ACPD
4, 753–803, 2004

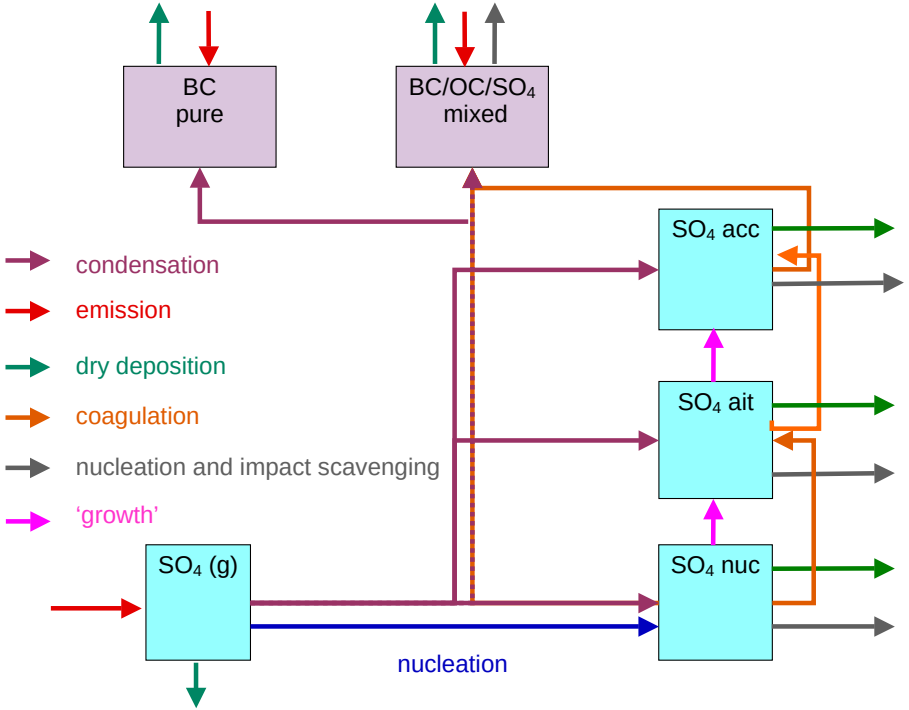

Fig. 1. Schematic picture of processes included in the aerosol model (after Wilson et al., 2001).

ACPD
4, 753–803, 2004

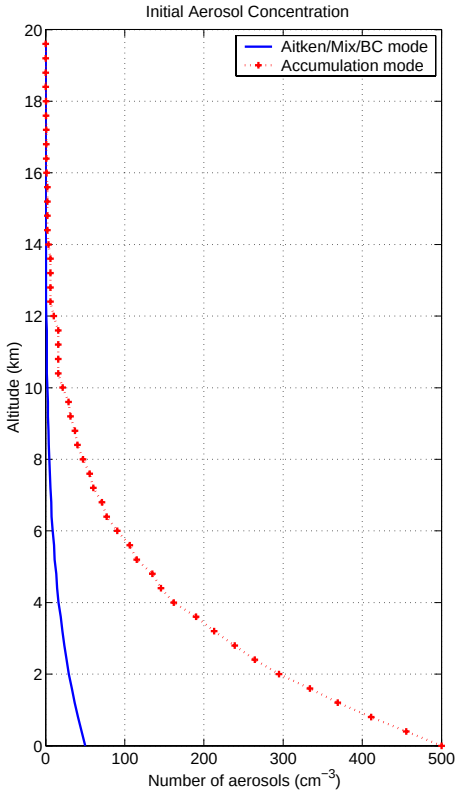

Fig. 2. Vertical profile of initial aerosol concentration.

ACPD
4, 753–803, 2004

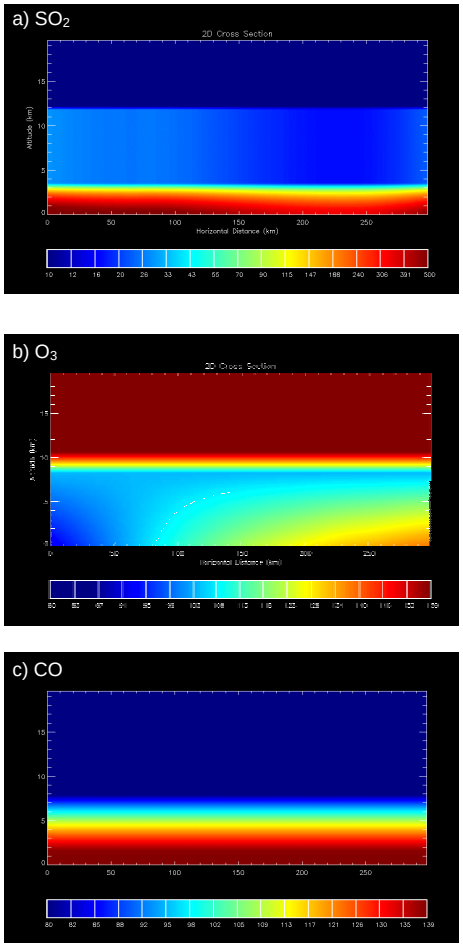

Fig. 3. Initial concentration for chemical compound **(a)** SO_2 (ppbv), **(b)** O_3 (ppbv), and **(c)** CO (ppbv).

ACPD
4, 753–803, 2004

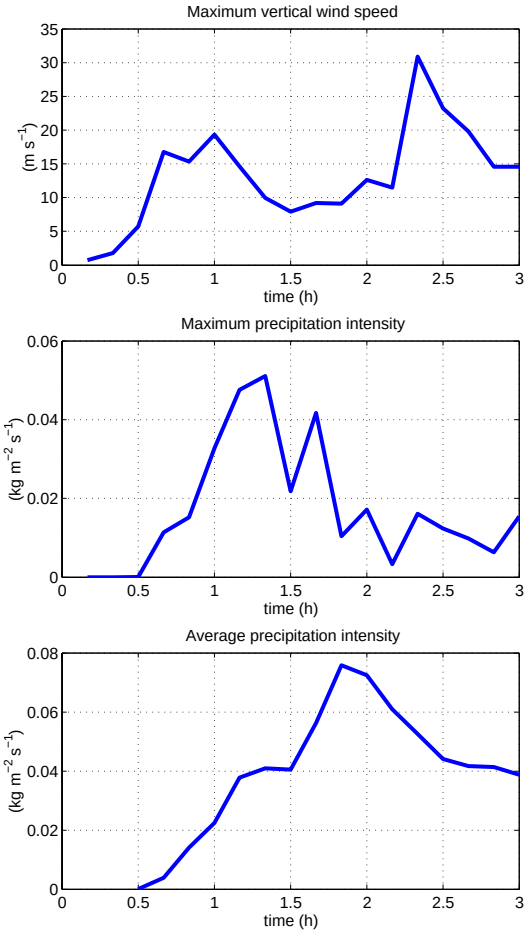

Fig. 4. Time development of simulated maximum vertical wind velocity, maximum precipitation and model domain average precipitation.

ACPD
4, 753–803, 2004

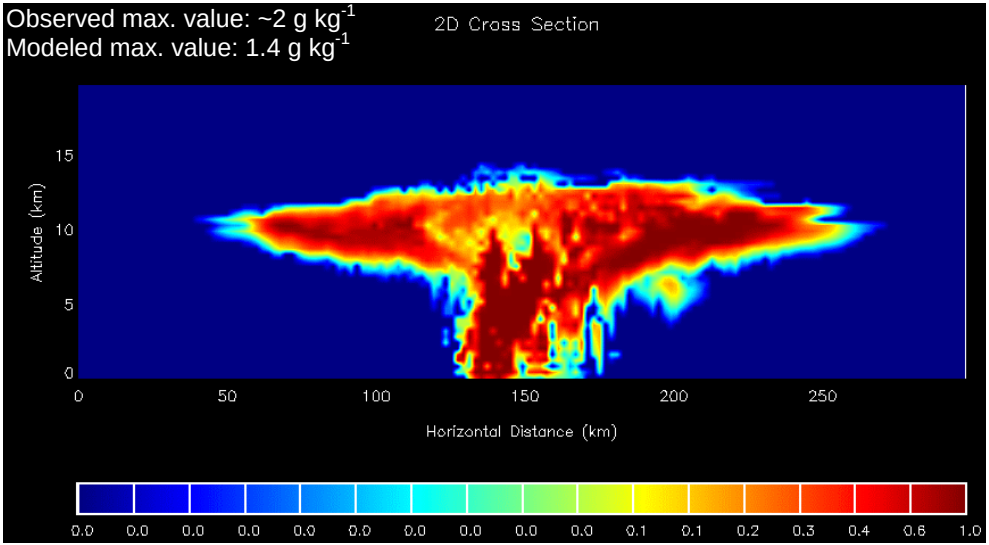

Fig. 5. (a) Modeled cloud water content (g kg^{-1}) after 3 h simulation. Observed and modeled values at 10.4 km are indicated in the figure.

ACPD
4, 753–803, 2004

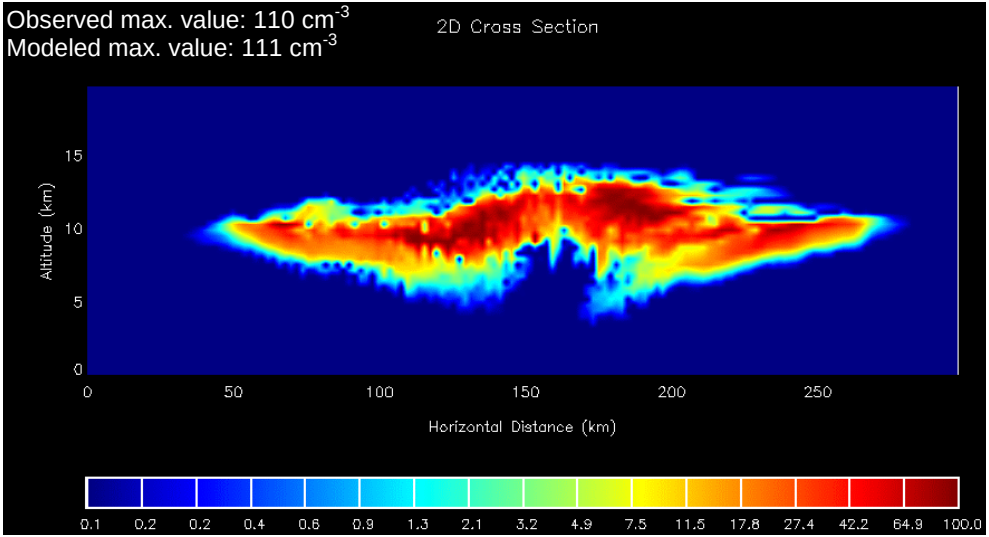

Fig. 5. (b) Modeled ice crystal number (cm^{-3}) after 3 h simulation. Observed and modeled values at 10.4 km are indicated in the figure.

ACPD
4, 753–803, 2004

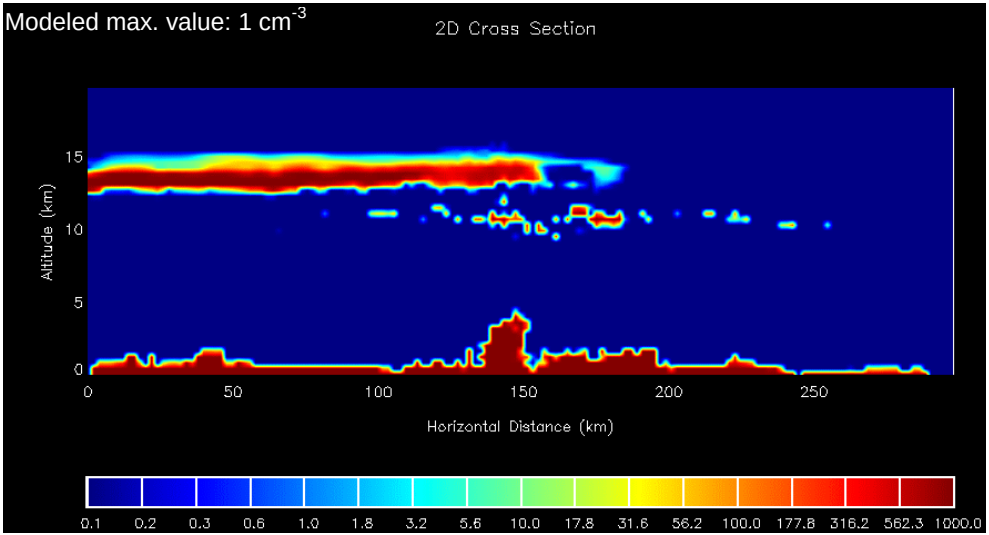

Fig. 5. (c) Modeled Nucleation Mode particle concentration (cm^{-3}) after 3 h simulation. The modeled value at 10.4 km is indicated in the figure.

ACPD
4, 753–803, 2004

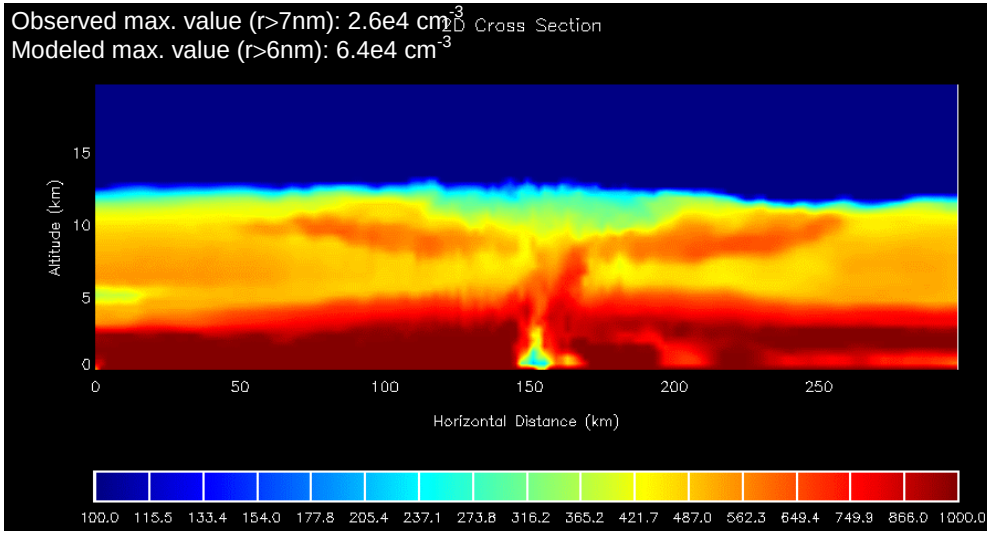

Fig. 5. (d) Modeled Aitken Mode particle concentration (in 100 cm^{-3}) after 3 h simulation. Modeled and observed values at 10.4 km are indicated in the figure.

ACPD
4, 753–803, 2004

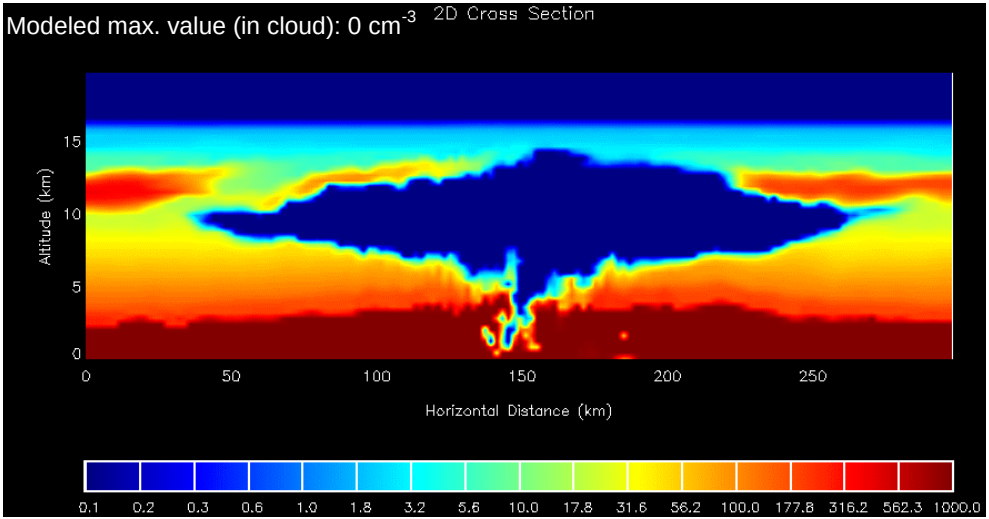

Fig. 5. **(e)** Modeled Accumulation Mode particle concentration (cm^{-3}) after 3 h simulation. Modeled and observed values at 10.4 km are indicated in the figure.

ACPD
4, 753–803, 2004

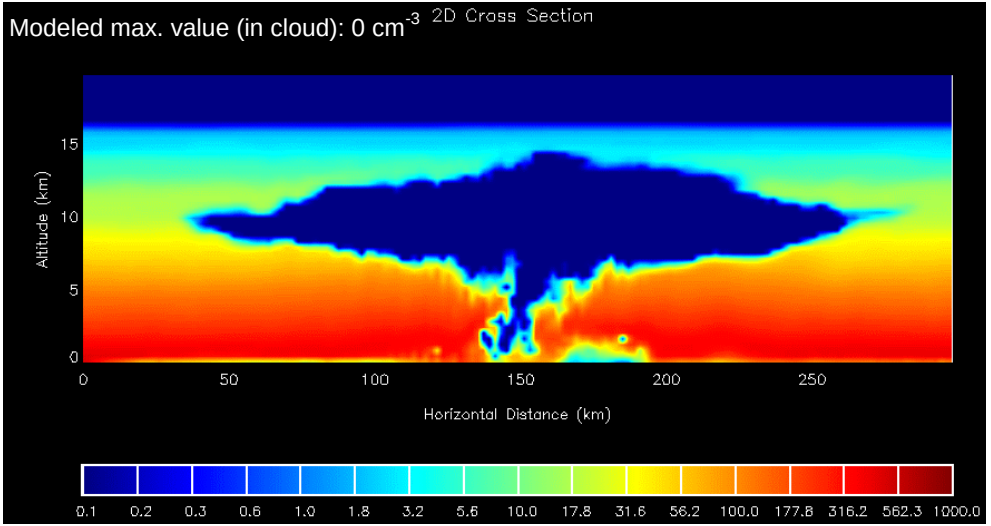

Fig. 5. (f) Modeled Mixed Mode particle concentration (cm^{-3}) after 3 h simulation. The modeled value at 10.4 km is indicated in the figure.

ACPD
4, 753–803, 2004

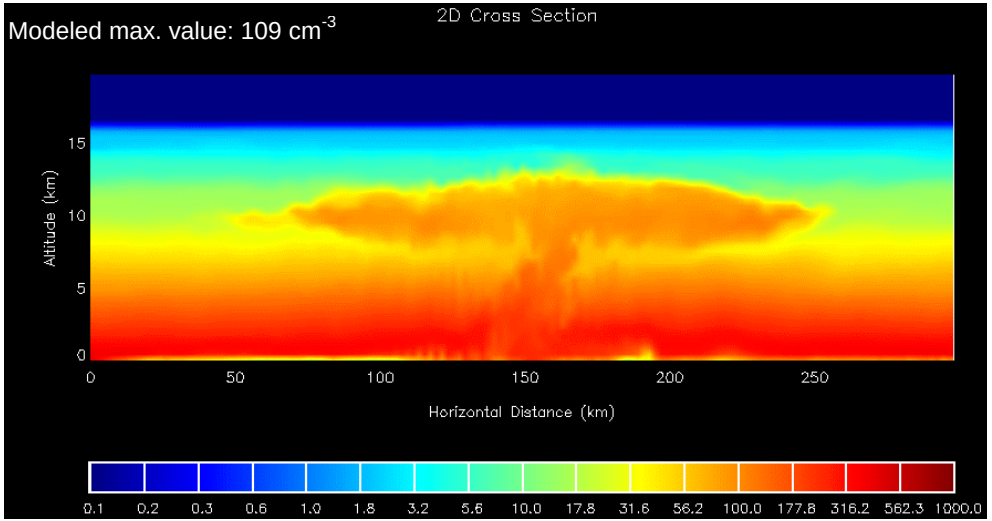

Fig. 5. (g) Modeled BC Mode particle concentration (cm^{-3}) after 3 h simulation. The modeled value at 10.4 km is indicated in the figure.

ACPD
4, 753–803, 2004

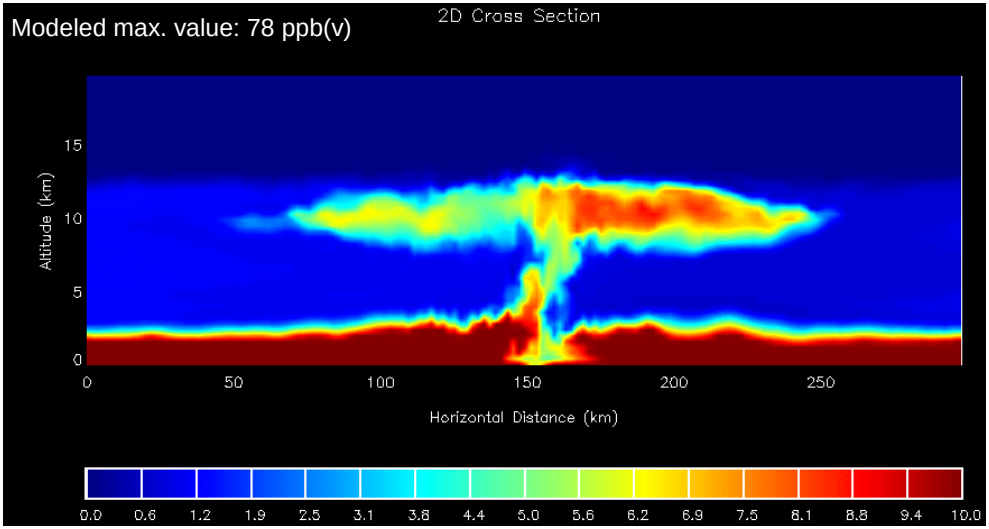

Fig. 5. (h) Modeled SO_2 concentration (ppbv) after 3 h simulation. The modeled value at 10.4 km is indicated in the figure.

ACPD
4, 753–803, 2004

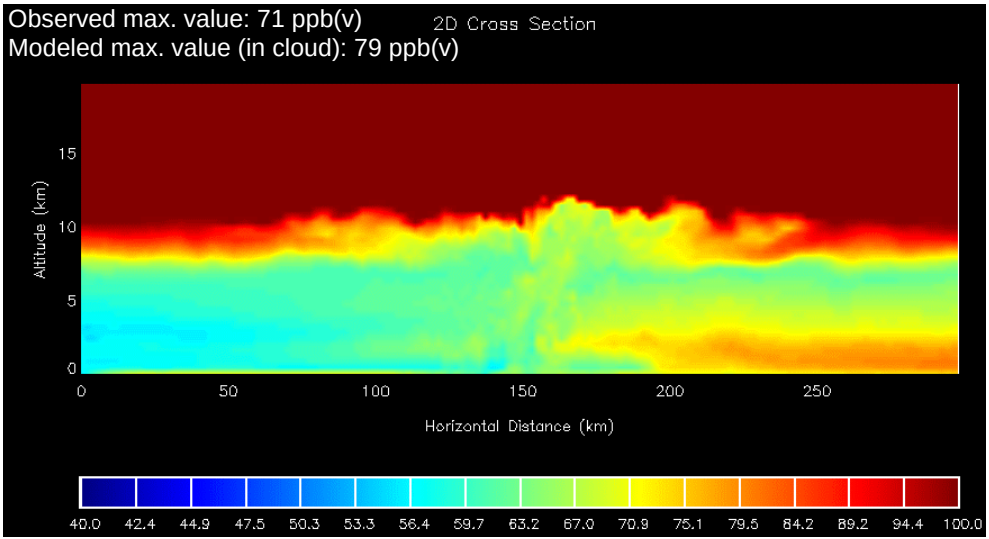

Fig. 5. (i) Modeled O_3 concentration (ppb) after 3 h simulation. Modeled and observed values at 10.4 km are indicated in the figure.

ACPD
4, 753–803, 2004

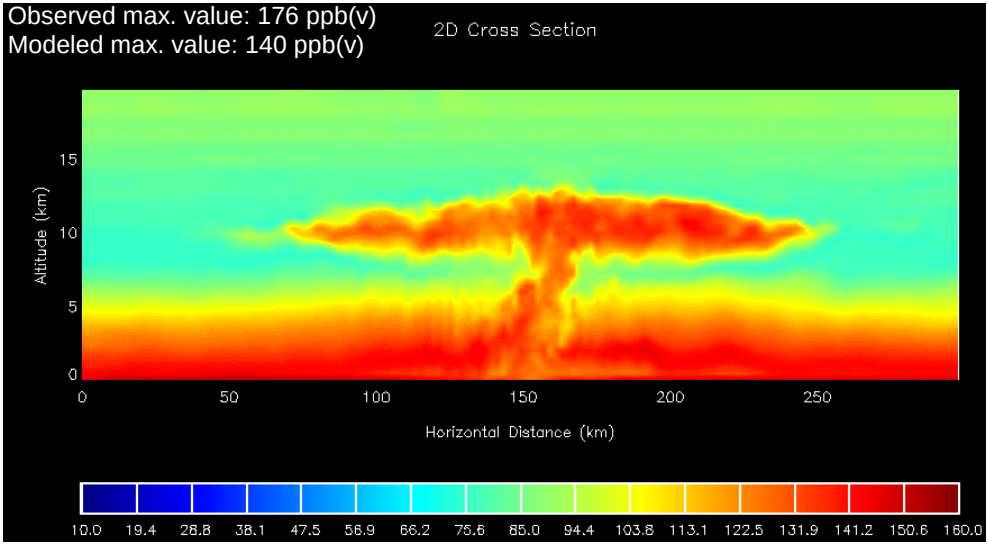

Fig. 5. (j) Modeled CO concentration (ppb) after 3 h simulation. Modeled and observed values at 10.4 km are indicated in the figure.

ACPD
4, 753–803, 2004

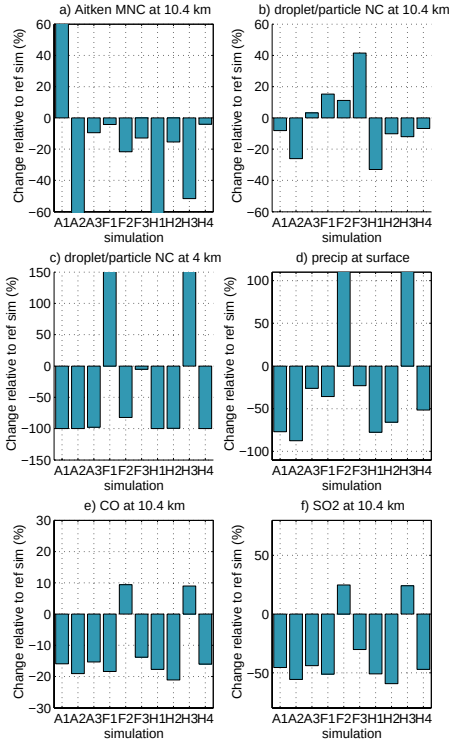

Fig. 6. Percentage difference at t = 3 h in **(a)** average Aitken mode particle number concentration at 10.4 km, **(b)** ice/droplet particle number concentration at 10.4 km, **(c)** ice/droplet particle number concentration at 10.4 km, **(d)** average surface precipitation, **(e)** average CO concentration at 10.4 km and **(f)** average SO_2 concentration between reference simulation and sensitivity simulation series A, F and H.

ACPD
4, 753–803, 2004

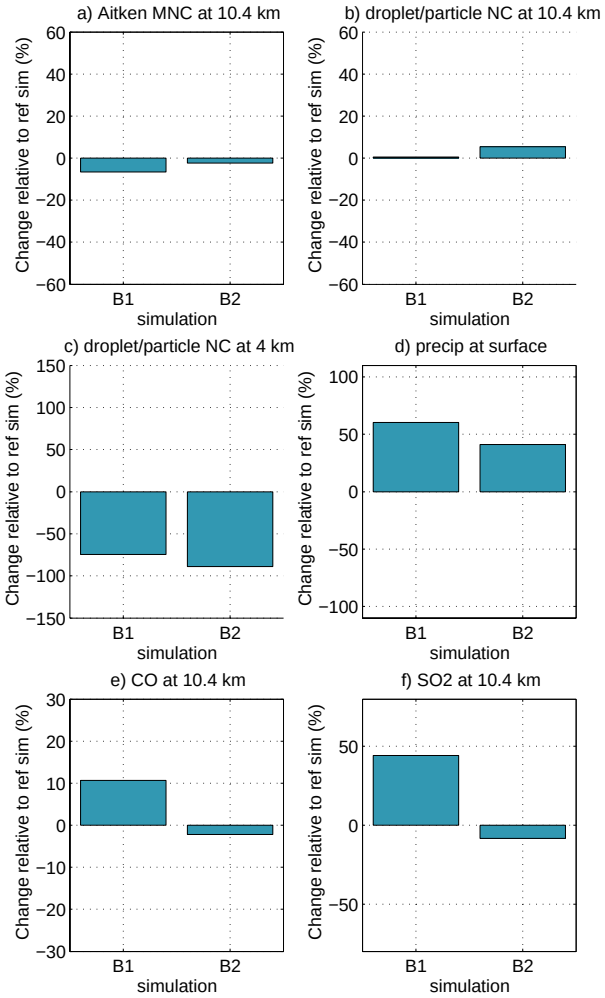

Fig. 7. Same as Fig. 6, but for sensitivity simulation series B.

ACPD
4, 753–803, 2004

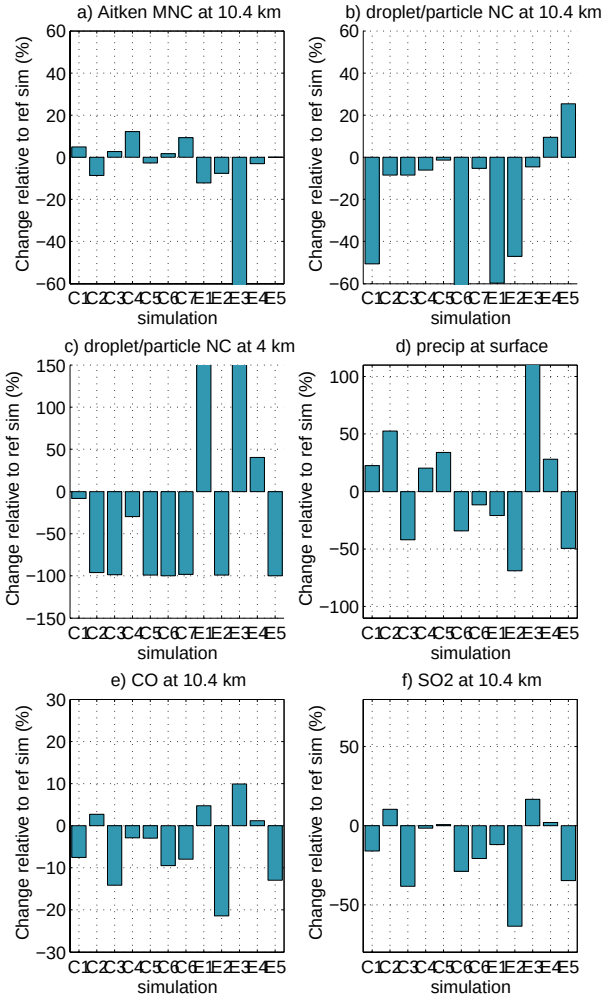

Fig. 8. Same as Fig. 6, but for sensitivity simulation series C and E.

ACPD
4, 753–803, 2004

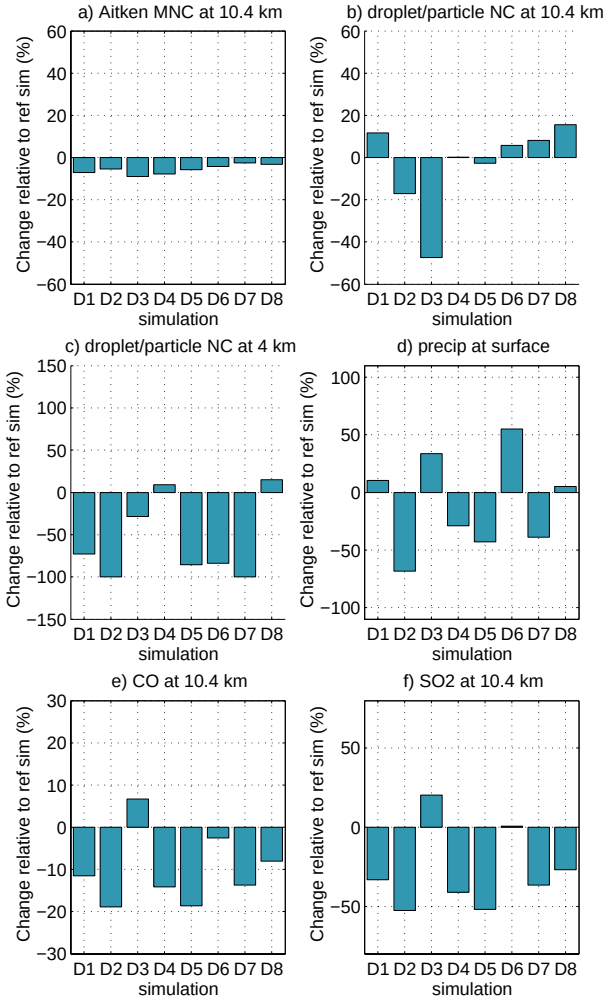

Fig. 9. Same as Fig. 6, but for sensitivity simulation series D.

ACPD
4, 753–803, 2004

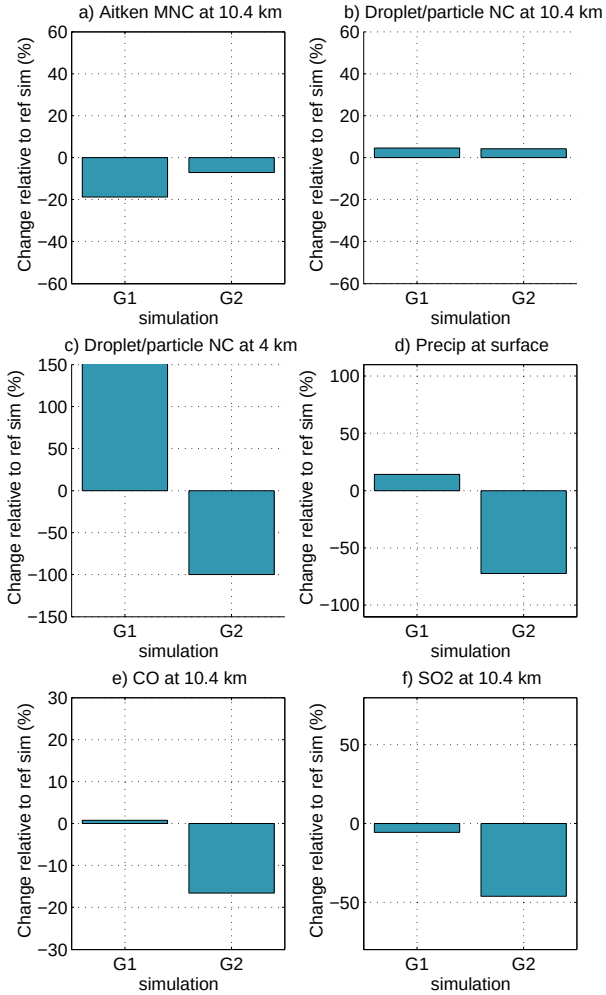

Fig. 10. Same as Fig. 6, but for sensitivity simulation series G.

ACPD
4, 753–803, 2004

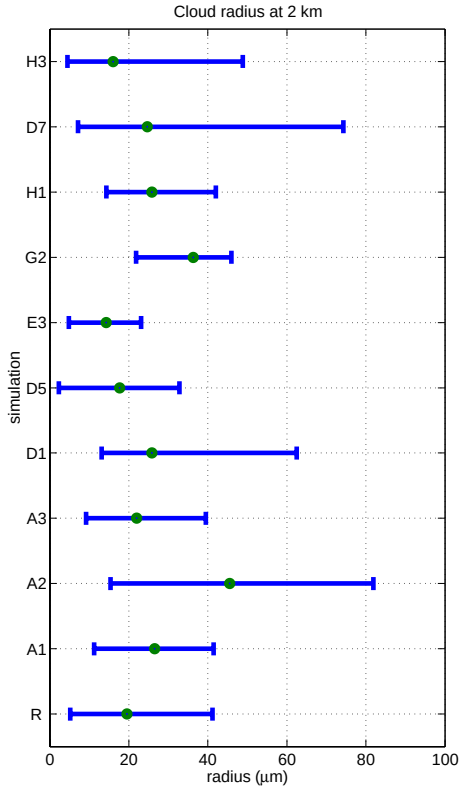

Fig. 11. (a) Average (both horizontally and over 3 h of simulation) effective cloud droplet radius at cloud base (2.0 km). Also shown in the figure are the maximum and minimum horizontally averaged effective cloud droplet radius simulated over the 3 h period.

ACPD
4, 753–803, 2004

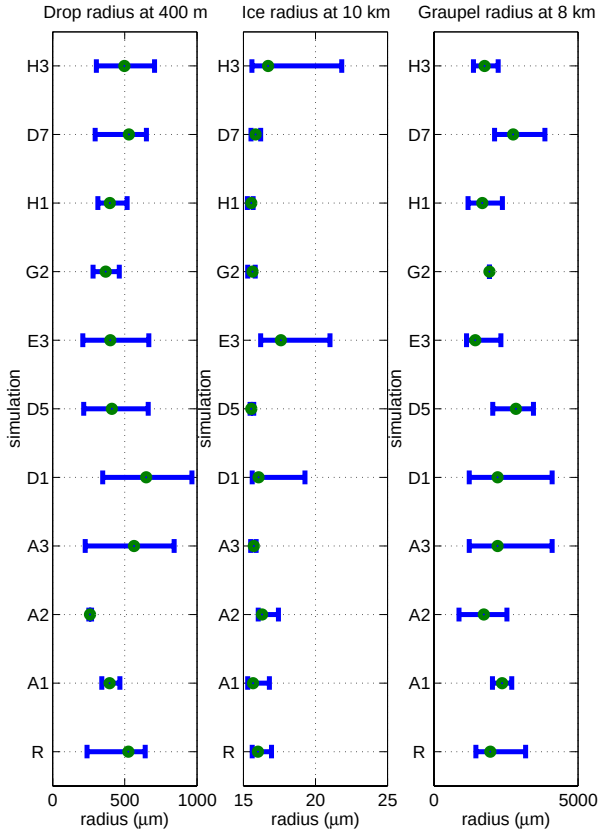

Fig. 11. (b) Average (both horizontally and over 3 h of simulation) effective rain droplet radius, ice particle radius and graupel radius at 400 m, 10 km and 8 km, respectively. Also shown in the figure are the maximum and minimum horizontally averaged effective radii simulated over the 3 h period.

ACPD
4, 753–803, 2004